600 GHz resonant mode in a parallel array of Josephson tunnel junctions connected by superconducting microstrip lines

Kaplunenko, V. K.; Larsen, Britt Hvolbæk; Mygind, Jesper; Pedersen, Niels Falsig

Published in:
Journal of Applied Physics

Link to article, DOI:
10.1063/1.357500

Publication date:
1994

Document Version
Publisher's PDF, also known as Version of record

600 GHz resonant mode in a parallel array of Josephson tunnel junctions connected by superconducting microstrip lines

V. K. Kaplunenko,[a] Britt H. Larsen, J. Mygind, and N. F. Pedersen
Physics Department, Technical University of Denmark, DK-2800 Lyngby, Denmark

(Received 11 March 1994; accepted for publication 17 May 1994)

The high frequency properties of the one-dimensional transmission line consisting of a parallel array of resistively shunted Josephson tunnel junctions have been studied in the limit of relatively low damping where this nonlinear system exhibits new and interesting phenomena. Here we report on experimental and numerical investigations of a resonant step observed at a voltage corresponding to 600 GHz in the dc current-voltage characteristic of a parallel array of 20 identical small $NbAl_2O_3Nb$ Josephson junctions interconnected by short sections of superconducting microstrip line. The junctions are mutually phase locked due to collective interaction with the line sections excited close to the half wavelength resonance. The phase locking range can be adjusted by means of an external dc magnetic field and the step size varies periodically with the magnetic field. The largest step corresponds to a superconducting phase difference of π between neighboring junctions.

I. INTRODUCTION

Superconducting transmission lines are often used as connecting and matching elements in Rapid Single Flux Quantum (RSFQ) logic.[1] The RSFQ transmission line, one of the vital RSFQ elements, is a parallel connection of shunted Josephson tunnel junctions typically with the McCumber parameter $\beta_c \approx 1$. A further requirement for such an array is that $I_cL/\Phi_0 \approx 1$, where I_c is a critical current of the junctions, L is the inductance connecting them and $\Phi_0 = h/2e$ is the flux quantum. Typically the discreteness parameter $\Lambda_j = L_j/L$ attains values of order 0.1–0.3. This makes fluxons well localized in the array. L_j is the intrinsic inductance of the Josephson junction.

Recently it was reported[2] that an overdamped array of junctions shows new dynamic states due to the non-uniform distribution of magnetic field within the array. This effect, it seems, is a common feature for the overdamped systems in the RSFQ family of base circuits. There may also be unanticipated effects caused by the high frequency properties of the interconnecting circuit elements such as for example the microstrip lines connecting the Josephson junctions in the RSFQ transmission line. Such effects are not expected to produce noticeable changes in the current-voltage (I-V) curve of an overdamped system, but may influence the repetition rate of fluxons, which is critical for logic devices.[1] In order to elucidate the influence of the inherent resonance frequencies it is useful to investigate an RSFQ circuit in the low damping limit, e.g., with all the shunting resistances removed.

Our investigation of 20-junction parallel arrays of underdamped junctions interconnected by resonant microstrip sections also provides new insight into the physics of discrete Josephson junction systems. For a discreteness parameter $\Lambda_j > 1$ the dynamics of such systems may be understood within the theory where the localized single fluxons are treated as free particles moving in a periodic potential.[3–7] We operate in a quite different range of parameters. Due to the fact that the microstrip line has a relatively high inductance, Λ_j typically is at least ten times smaller, but as both Λ_j and the damping can be varied in the experiments our investigation supplements the previously published work.

The phenomena described in this paper are closely related to the resonance modes excited in the microstrip lines connecting the Josephson junctions. Interactions between a short junction placed in the middle of an open-ended superconducting microstrip line was considered previously in Ref. 8 (see also references herein); interaction of two junctions through the normal metal microstrip line was investigated in Ref. 9, and in Ref. 10 the spatial distribution of standing waves in a superconducting transmission line with many short junctions was measured. The main difference between our experiments and those mentioned above is the presence of two kinds of coupling between the Josephson junctions: (i) the rf interaction between the junctions via the microstrip line (like Ref. 9) and (ii) the direct dc superconducting connection between the junctions through the superconducting inductance of the microstrip line. The latter means that the enclosed dc magnetic flux imposes controlled boundary conditions on the ends of the microstrip line. These two kinds of interactions are responsible for the observed resonance mode. Since Λ_j is somewhat smaller than one, the strongest interaction takes place for $I_cL/\Phi_0 \approx 1$.

II. FABRICATION TECHNIQUE

Standard trilayer Nb-AlO_x-Nb technique was employed to fabricate the 20-junction arrays with a critical current density of about 1 kA/cm^2. Figure 1 shows the layout of one cell of the array. The 4 μm diameter circular Josephson junctions are identical to within a few percent. Their characteristics at 4.2 K are the following: Critical current $I_c = 365$ μA, subgap junction resistance $R_j = 40$ Ω, normal state resistance

[a]Permanent address: Institute of Radio Engineering and Electronics, Mochovaya 11, Moscow 103907, Russia.

 0021-8979/94/76(5)/3172/5/$6.00

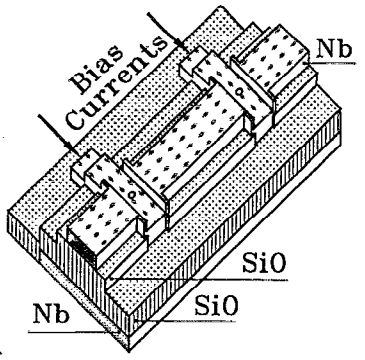

FIG. 1. Out-of-scale layout of one interferometer cell in the parallel current biased 20-junction array. In the regions close to the circular junctions the top and bottom Niobium electrodes are separated with a single SiO insulation layer. Between the junctions there are two layers of SiO. The distance between successive junctions is 110 μm and the length of the microstrip line is 85 μm.

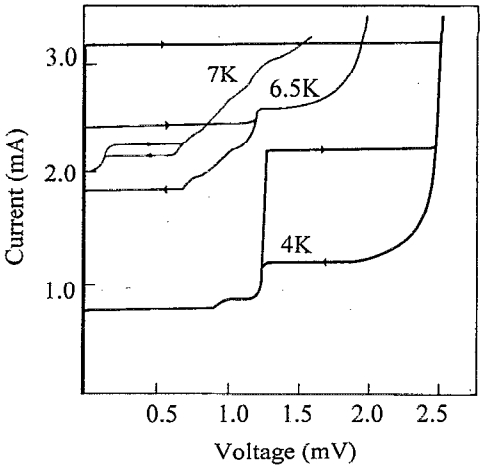

FIG. 3. Experimental I-V curves of the under-damped 20-junction array at different temperatures for fixed magnetic field chosen to maximize the size of the step near 600 GHz at 4 K.

$R_n=3.5\ \Omega$ ($R_j/R_n=11$). The junction capacitance is estimated to be $C_j=0.8$ pF,[11] giving a McCumber parameter $\beta_c=1400$. From the geometry of the electrode overlap the capacitance C_m of the microstrip line is calculated to be $C=0.10$ pF. The inductance L between neighboring junctions ($L_1 - L_{20}$ in Fig. 2), as measured with an overdamped two-junction interferometer located on the substrate close to the array, is $L=7.25$ pH.

Referring to Fig. 1 the microstrip line is formed between the top and bottom Nb electrode separated by the two SiO layers. The thickness of the Nb base film is 220 nm, the following two SiO layers both have a thickness of 200 nm, and finally the thickness of the top Nb electrode was 450 nm. The microstrip width was 10 μm. Using a relative permittivity $\epsilon=5.7$ which for our geometry and frequency gives an effective permittivity $\epsilon_{\text{eff}}=5.28$ we calculate a characteristic impedance of 6.0 Ω.[12]

III. EQUIVALENT CIRCUIT

Figure 2 shows the equivalent diagram of the circuit under investigation. The one-dimensional array consists of twenty Josephson tunnel junctions connected in parallel ($J_1 - J_{20}$). The unit cell is a two-junction interferometer (see also Fig. 1) sharing its junctions with the neighboring cell. The inductance, L, connecting the junctions consists of (i) the inductance of the microstrip line and (ii) two small inductances of the top film above the single SiO layer located between the microstrip line and the junction. The value of these small inductances was calculated to contribute with about 10% of L. There are two bias currents supplied to the array. I_b is a uniformly distributed current applied to the individual junctions through the resistances $R_1 - R_{20}$. These currents are indicated with arrows in Fig. 1. A magnetic field can be introduced by injecting a current I_h to the edge junction (J_1) and subtracting the same current from the other edge junction (J_{20}). The array voltage, V, was measured across one of the edge junctions.

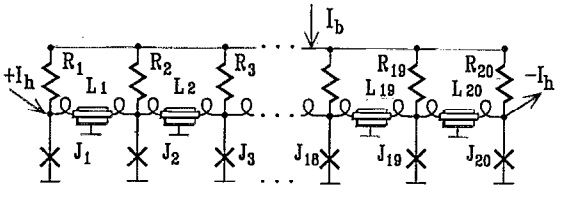

FIG. 2. Equivalent circuit of the one-dimensional array of 20 under-damped Josephson tunnel junctions. I_b is the uniformly distributed dc bias current. The injected edge currents $\pm I_h$ are used to produce a magnetic field inside the array. The array voltage, V, is measured across one of the edge junctions.

IV. EXPERIMENTAL RESULTS

Figure 3 shows a series of experimental V vs I_b curves obtained at different temperatures with fixed I_h. At 4 K there is a large step of nearly constant voltage at a voltage corresponding to 600 GHz. This step is very stable and reproducible for all samples with the same geometry. The lowest value of the differential resistance, R_d, on this step is about 0.03 Ω. At a higher temperature this resonance mode still exists but the step size is significantly reduced and finally at 7 K ($T/T_c=0.76$) an additional resonance appears at 0.16 mV corresponding to a frequency of 77 GHz. Throughout the measurement the current I_h is kept constant at the value which maximizes the step size at 4 K.

The nature of these steps may be understood from an evaluation of the possible resonance frequencies of the system. For the unloaded resonator formed by the superconducting microstrip line the resonance frequencies can be found from $f=c/(2\ l\ \sqrt{\epsilon\chi})$, where l is the length of the resonator, ϵ is the permittivity of SiO, and $\chi=(d+2\lambda)/d$ accounts for the penetration of the magnetic field into the resonator electrodes. Here c is the free-space light velocity, λ is the London penetration depth for the Nb films, and d is the total thickness of the two SiO layers. Taking $\epsilon=\epsilon_{\text{eff}}=5.28$ as mentioned above and $\lambda=90$ nm we find for $l=110\,\mu$m the resonance frequency to be $f=493$ GHz. If instead we use $l=85\,\mu$m we get $f=637$ GHz which is much closer to the experimental value. This indicates that (despite the fact that

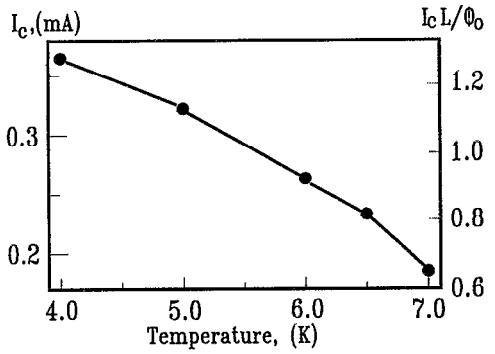

FIG. 4. Temperature dependence of the critical current of a single junction in the array.

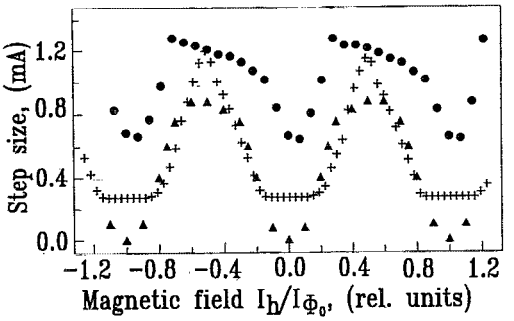

FIG. 5. Experimental (full dots and crosses) and simulated (triangles) data for the height of the 600 GHz step vs the applied magnetic field. In the plot of the experimental data we used $I_{\Phi_0}=\Phi_0/L=0.286$ mA obtained by an independent measurement of the inductance $L=7.25$ pH. The actual size of the symbols corresponds approximately to the accuracy of both measurements and simulations.

the distance between the junctions is 110 μm) only the part of the microstrip line where both the two SiO layers are present (see Fig. 1) is responsible for the observed 600 GHz resonance mode. In this rather rough calculation no corrections were made for the loading of the resonator by the junction impedance.[8] The inductance of a single interferometer loop including the area of the microstrip line array is estimated to be $L=7.25$ pH. With the capacitance of one junction, $C_j=0.8$ pF we can calculate the ordinary LC-resonance frequency for our array as $f=1/(2\pi\sqrt{LC_j})=66$ GHz. This is close to the observed resonance at 7 K and the small discrepancy might be due to the crude estimation of the junction capacitance.

Figure 4 depicts the temperature dependence of the critical current I_c for a single junction. Because of the resonances it was impossible to measure directly the critical current of the un-shunted array. Instead the 4 K value in Fig. 4 was measured on shunted two junction interferometers placed elsewhere on the same chip, and then scaled to the 20-junction array. The temperature dependence of I_c is established by measuring the temperature dependence of the quasiparticle jump at the gap voltage. In Fig. 4 is also plotted the well known RSFQ parameter $\eta=I_cL/\Phi_0=1/(2\pi\Lambda_j)$, which gives how many states with different number of fluxons are available for the interferometer. Comparing Figs. 3 and 4 one can see that the 600 GHz mode exists when $\eta\approx1$ corresponding to $\Lambda_j\approx0.16$. Physically this means that a single fluxon in an interferometer should produce a circulating current comparable to the junction critical current. This is a first hint that localized fluxons are responsible for the high frequency resonance. At higher temperature both the critical current and the junction resistance decreases as seen in Fig. 3. At $T=7$ K, $\eta=0.65$, and $\Lambda_j=0.25$ which is enough to suppress the 600 GHz mode almost completely but the low frequency mode that typically exists at $\Lambda_j\geqslant1$ 3–7 is observed.

Further evidence that fluxons are responsible for the high frequency mode is the magnetic field dependence of the size of the 600 GHz step plotted in Fig. 5. In all experiments with several samples we observe a periodic dependence of the step size versus applied magnetic field. The period corresponds exactly to the introduction of one extra flux quantum per unit cell. Unfortunately the size of the array (about 2 mm) is too large to completely prevent the influence of parasitic magnetic flux trapped in the array. That is why the shape of the experimental curves in Fig. 5 depends on the thermal cycling.

V. RSFQ TRANSMISSION LINE MODEL AND SIMULATION RESULTS

Transmission lines can be modeled in several ways;[12] a fast method for computer simulation has been devised in Ref. 13. In this paper we used a simple one-dimensional transmission line model[12] consisting of a lumped element circuit with a large number of elements for the microstrip line present in each unit cell of the RSFQ transmission line. For the Josephson junctions the standard nonlinear-resistive (RSJN) model (see e.g., Ref. 14) was employed.

In order to limit the total number of elements a special simulation procedure was developed for the RSFQ transmission line unit cell having a two-junction interferometer with a lossless transmission line. In a preliminary simulation the Josephson junctions had the same capacitance as the lumped capacitances in the transmission line model in order to obtain perfect matching. These simulations showed a whole series of steps in the I-V curve, and their voltage position as expected strictly scales with the number of used lumped elements.

As a result of this preliminary simulation we have found an appropriate circuit model for the experimental microstrip line. It consists of a lossless transmission line that comprises 29 capacitances with $c=0.01$ pF and 28 inductances with $l=0.237$ pH. The characteristic impedance of the line is $Z_s=4.7\ \Omega$ which is close to the value estimated from the experiment $Z_e=6.0\ \Omega$. The total inductance of the line including the two inductances (0.53 pH each) connecting the microstrip line to the junctions (see Fig. 1) is 7.7 pH, which is also close to the experimental value.

The total model circuit comprises 1141 elements and 571 nodes in which the quantum mechanical phase is simulated. The simulation was done on a Silicon Graphics computer and was based on our own ANSI C compatible software. The RSJN model junction parameters were chosen to be close to

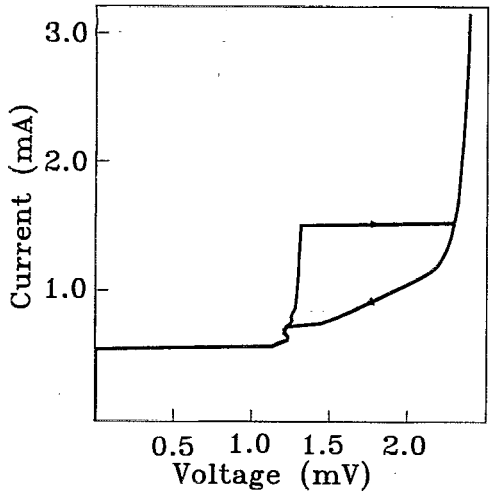

FIG. 6. Simulated I-V curve of the one-dimensional under-damped array with an applied magnetic field corresponding to one fluxon enclosed per two cells or a π superconducting phase difference between neighboring junctions, $I_h/I_{\Phi_0}=0.5$.

the experimental values: critical current is $I_c=0.375$ mA; the junction resistance below the gap is $R_j=40\ \Omega$ and above the gap $R_n=4.0\ \Omega$, giving $R_j/R_n=10$; finally the junction capacitance is $C_j=0.74$ pF.

The result of a simulation of the I-V curve of this array is presented in Fig. 6. Note the good agreement with the experimental results in Fig. 3. The simulated dependence of the step size versus magnetic field included in Fig. 5 also shows fine agreement with the experimental data.

In order to clarify the dynamics that give rise to the observed high frequency mode, we plot in Fig. 7 the simulated instantaneous voltages across each of the 20 junctions as a function of time and at different values of the applied magnetic field. The average voltage of each junction is the same and equals the 600 GHz step voltage. The magnetic field produces half a fluxon per cell in Fig. 7(a) corresponding to the maximum step size. In Fig. 7(b) the magnetic field produces a quarter of fluxon per cell. The simulation shows

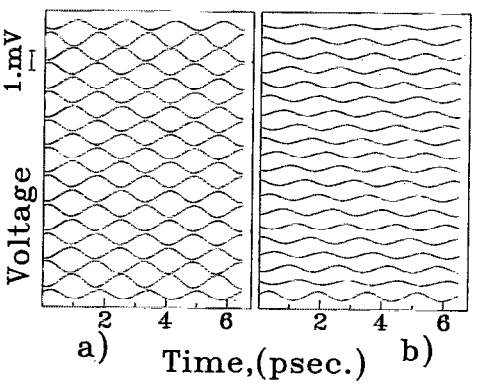

FIG. 7. Instantaneous voltages across the all 20 junctions in sequence. The average voltage corresponds to the 600 GHz step. For clarity the curves are off-set vertically. (a) $I_h/I_{\Phi_0}=0.5$, $I_b=1.35$ mA; (b) $I_h/I_{\Phi_0}=0.25$, $I_b=1.025$ mA.

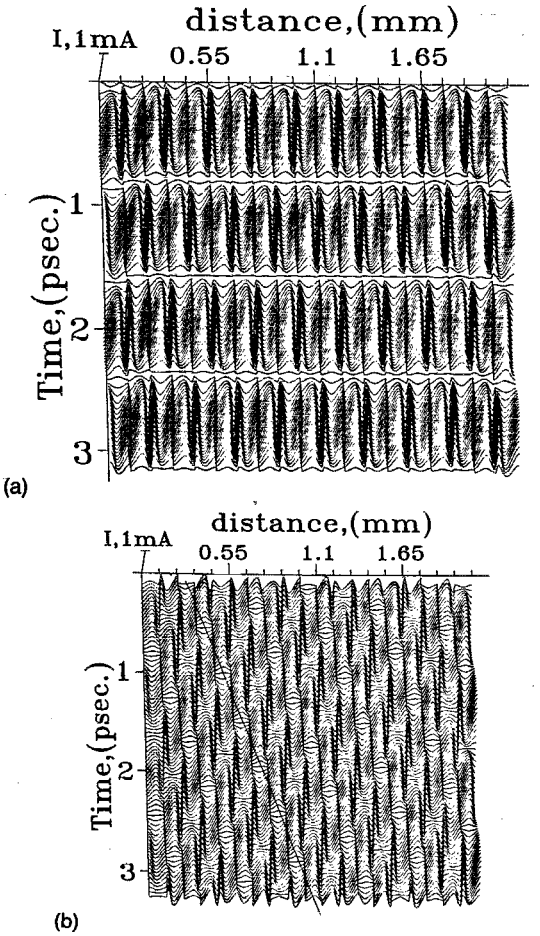

FIG. 8. Spatial distribution of the instantaneous current along the array as function of time. The distance between successive junctions is 110 μm and the small dial marks indicate the junction positions. (a) $I_h/I_{\Phi_0}=0.5$, $I_b=1.35$ mA; (b) $I_h/I_{\Phi_0}=0.25$, $I_b=1.025$ mA.

that the magnetic field strictly sets the superconducting phase difference between neighboring junctions. One can see also that the high frequency amplitude can be tuned with the applied magnetic field.

Figure 8 shows the time evolution of the instantaneous spatial distribution of the longitudinal current in the array. Clearly one can see that independent of the magnetic field there is a standing wave excited in the microstrip line between the Josephson junctions. This result confirms our evaluation of the resonance frequency given under the discussion of the experimental results. Figure 8(a), with $I_h/I_{\Phi_0}=0.5$, shows that the amplitude of the instantaneous longitudinal current becomes zero for all cells simultaneously; this means that the capacitances of neighboring junctions are completely charged and no currents flow through the junctions. The magnetic field produces a phase difference of π between neighboring junctions and every fluxon moves simultaneously to the next cell.

When the magnetic field corresponds to a $\pi/2$ phase difference [Fig. 8(b)], the capacitances are charged sequentially producing a charge wave, as can be seen when following the solid line in Fig. 8(b). The velocity of this wave can be much higher than the velocity of light because it is a

phase velocity without real physical significance. In this case the fluxons sequentially push one another producing a fluxon density wave similar to that described in Ref. 15. In our case one should interpret the term fluxon as a fixed value of the superconducting phase moving along the array. As obvious from Fig. 8 its shape is strongly deformed by the rf currents.

In simple terms we may formulate the main result of the simulation as follows: The Josephson junctions, which are coupled by means of the superconducting microstrip lines, have a fixed average superconducting phase difference between them as set by the applied magnetic field. In principle small oscillations of the phase near this average value are possible, but in the presence of the standing wave in the microstrip line the high frequency impedance of this line (including the coupling inductances and the junction reactances) goes to zero and completely phase-locks the junctions.

VI. CONCLUSIONS

We have found both experimentally and from computer simulations a high frequency mode in an array of underdamped junctions current biased in parallel. Despite the excitation of a standing wave in the microstrip lines between the junctions, the whole dynamics is a resonant propagation of fluxons through the array. The velocity of this propagating mode is extremely high and equals the velocity of electromagnetic waves in the SiO layer. One may ignore the junction capacitances which are ten times larger than the lumped microstrip model capacitances. The dynamics is in many ways similar to the well known flux flow oscillator (FFO) and it may be possible to utilize this system as a stable high frequency generator. A possible limitation for the practical use of the device may be losses in the niobium/SiO transmission lines at very high frequencies.[16,17] This problem deserves further study.

ACKNOWLEDGMENTS

The samples were fabricated in the IRE Technology Group headed by V. P. Koshelets. We also thank Olga V. Kaplunenko and S. Kovtonuk who fabricated the circuits, and A. V. Ustinov, J. Niemeyer, and P. Guttmann for fruitful discussions. This work was partially supported by the Danish Research Academy, NORPAS, and NATO Linkage Grant (LG 921040).

[1] K. K. Likharev and V. K. Semenov, IEEE Trans. Appl. Supercond. **1**, 13 (1991).
[2] V. K. Kaplunenko, E. B. Goldobin, M. I. Khabipov, B. H. Larsen, J. Mygind, and N. F. Pedersen, J. Appl. Phys. **74**, 5854 (1993).
[3] A. V. Ustinov, M. Cirillo, and B. A. Malomed, Phys. Rev. B **47**, 8357 (1993).
[4] M. Cirillo, B. H. Larsen, A. V. Ustinov, V. Merlo, V. A. Oboznov, and R. Leoni, Phys. Lett. A **183**, 383 (1993).
[5] A. V. Ustinov, B. H. Larsen, and M. Cirillo, in *Applied Superconductivity*, edited by H. C. Freyhardt (DGM Informationsgesellschaft, Germany, 1993), pp. 1343–46.
[6] E. H. Visscher, J. van der Eyden, P. Hadley, and J. E. Mooij, Physica B **194–196**, 1667 (1994).
[7] H. S. J. van der Zant, D. Berman, T. P. Orlando, and K. A. Delin (unpublished).
[8] A. Larsen, H. Dalsgaard Jensen, and J. Mygind, Phys. Rev. B **43**, 10179 (1991).
[9] H. J. T. Smith, J. A. Blackburn, and N. Grønbech-Jensen, J. Appl. Phys. **74**, 5101 (1993).
[10] D. Quenter, S. Stehle, T. Doderer, C. A. Krulle, R. P. Huebener, F. Mueller, J. Niemeyer, R. Popel, P. Weimann, R. Ruby, and A. T. Barfknecht, Appl. Phys. Lett. **63**, 2135 (1993).
[11] V. P. Koshelets, S. A. Kovtonyuk, I. L. Serpuchenko, L. V. Filippenko, and A. V. Shchukin, IEEE Trans. Magn. **MAG-27**, 3141 (1990).
[12] B. C. Wadell, *Transmission Line Design Handbook* (Artech House, New York, 1991), p. 94.
[13] M. Morisue, S. Hayashi, A. Kanasugi, and T. Van Duzer, IEEE Trans. Magn. **MAG-27**, 2906 (1991).
[14] K. K. Likharev, *Dynamics of Josephson Junctions and Circuits* (Gordon and Breach, Philadelphia, PA, 1991), p. 48.
[15] O. H. Olsen, A. V. Ustinov, and N. F. Pedersen, Phys. Rev. B **48**, 13133 (1993).
[16] R. L. Kautz, J. Appl. Phys. **49**, 308 (1978).
[17] M. M. T. M. Dierichs, B. J. Feenstra, A. Skalare, C. E. Honingh, J. Mees, H. v. d. Stadt, and T. de Graauw, Appl. Phys. Lett. **63**, 249 (1993).